

Simulation of a Multimodal Wireless Remote Control System for Underwater Vehicles

Filippo Campagnaro[§], Federico Guerra[§], Federico Favaro[§]
Violeta Sanjuan Calzado[#], Pedro Forero^{*}, Michele Zorzi[§], Paolo Casari[‡]

[§]Department of Information Engineering, University of Padova, Italy

[#]NATO STO Centre for Maritime Research and Experimentation, La Spezia, Italy

^{*}US Navy Space and Naval Warfare Systems Center Pacific (SPAWAR), San Diego, CA, USA

[‡]IMDEA Networks Institute, Madrid, Spain

ABSTRACT

While the design of reliable and enduring remotely operated vehicles for underwater operations is currently a hot research area, there are not many options to control these systems in real time using wireless telemetry. In particular, a reliable, fully wireless control method that exploits state-of-the-art underwater wireless communication technologies is still lacking. In this paper, we consider the design and engineering of one such multimodal control system comprising optical and acoustic underwater communications, and characterize its performance under different configurations of the communication protocol stack. Compared to previous work, we introduce a proactive mechanism to switch among the components of the multimodal system by means of a signaling mechanism that requires negligible overhead. Our results suggest that a multimodal wireless control system can provide satisfactory control performance by supplying different levels of interaction with the vehicle, depending on the technology in use, and by reliably and timely switching between the available communication technologies.

Categories and Subject Descriptors

I.6.6 [Cooperative Underwater Communications]: Simulation and Modeling—*Simulation Output Analysis*; C.2.0 [Communication/Networking and Information Technology]: General—*Data communications*

General Terms

Design, Measurement, Performance

Keywords

Underwater acoustic communications, underwater optical communications, multimodal communications, ROV, wireless remote control, DESERT Underwater

Permission to make digital or hard copies of all or part of this work for personal or classroom use is granted without fee provided that copies are not made or distributed for profit or commercial advantage and that copies bear this notice and the full citation on the first page. To copy otherwise, to republish, to post on servers or to redistribute to lists, requires prior specific permission and/or a fee.

WUWNet'15, October 22 - 24 2015, Washington, DC, USA

Copyright 2015 ACM XXX-X-XXXX-XXXX-XX/XX/XX ...\$15.00.

1. INTRODUCTION AND RELATED WORK

The impending exploitation of non-acoustic underwater communication systems, including optical [1–4], electromagnetic [5, 6] and magneto-inductive [7] technologies, and the proliferation of Autonomous Underwater Vehicles (AUVs), are opening scenarios where static and mobile nodes are networked and interact via hybrid, multimodal communications. This may involve not only optical, acoustic and RF communications, but also different implementations of either technology, such as multiple acoustic modems working at different carrier frequencies, e.g., [8, 9]. Multimodal underwater communication networks have become a hot research topic, due to the advantages they can provide in several applications. For instance, in [10, 11], the authors propose a multimodal optical and acoustic system where an AUV patrols a network to retrieve a large amount of incoming data from static nodes. There, the focus is on the data retrieval mechanism and its performance rather than on remote control aspects. In [12], the authors report a first evaluation of a hybrid opto/acoustic system for AUVs swarms, where the acoustic modem is used for transmitting data, while the optical modem is employed to improve the effectiveness of the acoustic communication protocols by offering a higher data rate for signaling messages. The optical modem is currently under implementation.

Nowadays, Remotely Operated Vehicles (ROVs) [13–15] and Autonomous Underwater Vehicles (AUVs) [16] are widely used in order to monitor the underwater environment and execute different types of operations. For instance, ROVs are employed to defuse bombs, or to inspect pipelines, both in normal situations and in the presence of severe damage. The control of ROVs without deploying a connection via the so-called umbilical cable is a very interesting topic, both for research and for industrial applications. Although the umbilical makes it possible to manage the system in real time, it limits the mobility of the ROV due to cable strain and entanglement risks. Wireless ROV control would help avoid such issues by removing the need for a physical cable, at the price of an increased need for ROV power autonomy and smaller data rates. In this paper, we propose and simulate a possible implementation of a multimodal acoustic and optical fully-wireless remote control for underwater equipment. The feasibility of a single-mode version of such system, with no multi-modal capabilities, has been analyzed in [17]. In [18], the authors presented a Semi Immersible Unmanned Sur-

face Vehicle (SI-USV), radio-controlled from the ground, air, satellite and sea also during the semi-immersible operations. This system uses radio or satellite links to communicate with the remote controller, and can be employed only in very shallow water contexts, where the water depth is generally less than 10 m, due to the large attenuation suffered by electromagnetic waves under water. In any event [18] presents a notable attempt to implement a single-mode fully wireless remote control system, albeit limited to very shallow water scenarios. In [19], the authors envision a heterogeneous system where static nodes, AUVs and Autonomous Surface Vehicles (ASVs) cooperate to support marine operations. In particular, a centralized node collects the position of all the mobile nodes and instructs them to move towards a new way-point, by employing simple acoustic messages. The goal of this work is to employ a single-mode, erratic and event-based position control system, in order to coordinate the movement of static and mobile nodes. In contrast to [18] and [19], we present a multimodal remote control system for underwater vehicles that can work independently of the water depth by leveraging on different technologies for underwater communications, and is designed for quasi-real time communications between a controller and a vehicle. Our simulations show that our system effectively allows the link between the controller and the vehicle to exploit the maximum bit rate allowed by a given distance between the two parties, and to promptly switch to alternative communication systems when the channel conditions so require.

The contribution of this paper is twofold: first, in Section 2, we present the available communication technologies, defining the constraints and operational modes of a fully wireless remote control system; then, we implement the complete multimodal system in a network simulator, paying particular attention to the switching policy among multiple physical layers. In [10], the authors presented a switching algorithm based on the received power, designed in order to avoid any additional overhead; this design choice may result in a delayed switch between multiple communication technologies, hence in data losses or waste of bandwidth. In Section 2.1, we introduce a novel switching mechanism, to make the system more reactive. The simulation parameters and settings are presented in Section 3, including a description of the protocol stack. In Section 4, we report the performance of the designed system, with and without signaling mechanism and comparing the behavior of two different MAC layers: CSMA and TDMA. Finally, Section 5 draws some concluding remarks.

2. SYSTEM CONFIGURATION

We consider the task of remotely controlling the movement of an ROV along an eight-shaped trajectory over a $200 \text{ m} \times 300 \text{ m}$ area, where the controller is centrally placed. The trajectory is described by its x - y coordinates through the equations $x(t) = 100 \cos(t)$, $y(t) = 150 \sin(2t)$, where both $x(t)$ and $y(t)$ are in meters and $t \in [0, 2\pi]$. The depth of the ROV is fixed at 40 m from the surface. The controller commands the ROV along the trajectory through N_w subsequent waypoints, whose coordinates (x_k, y_k) are determined by computing $x(t)$ and $y(t)$ for $t = \frac{2\pi}{N_w}k$, $k = 1, \dots, N_w$. The controller transmits each waypoint to the ROV after a time $t_w(k) + t_g$ from the previous waypoint, where t_g is a guard time (set to 2.5 s in this work), $t_w(k) =$

$\frac{1}{v_R} \sqrt{(x_k - x_{k-1})^2 + (y_k - y_{k-1})^2}$ is the time required by the ROV to cover the distance between points (x_{k-1}, y_{k-1}) and (x_k, y_k) , and $(x_0, y_0) = (100, 0)$. In the following, we assume that the ROV's speed is fixed to $v_R = 1 \text{ m/s}$.

The trajectory described above has a maximum distance of about 180 m between the controller and the ROV. Three different communication technologies, one optical and two acoustic, are brought together to construct a multimodal controller. Each technology has its own specific data communication rate and reliable transmission ranges, thus, it is necessary to devise a switching system able to choose the best technology to use as a function of range during the operation of the remote control system.

Due to the different communication rates, the multimodal remote control system can provide different monitoring quality service depending on the position of the ROV. Such quality may change widely when switching from optical communications to different acoustic communication systems, and may range from full control including high-quality video to progressively lower control levels implying, e.g., low-quality video, low-quality image slide shows, down to simple movement commands. In light of the analysis carried out in [17], we can define the following modes of operation in order of decreasing quality of the control experience [20]:

- **Mode HD** provides full control capabilities (movement, ROV tools, etc.) and comprehensive feedback from the ROV, including a HD-quality video streaming from the ROV to the controller; the required bit rate for this service level is on the order of 1.4 Mbps;
- **Mode 3** maintains full control over the ROV movement and tools, but entails a significant decrease of the video quality, so that the required bit rate decreases to 66 kbps;
- **Mode 2** downgrades the video streaming into the transmission of an image slide-show, and requires a bit rate of 48 kbps;
- **Mode 1** further downgrades the quality of the image slide-show, and requires a bit rate of 30 kbps [20];
- **Mode 0** drops video streaming and maintains only the mandatory control of the movement and of the tools of the ROV, thus requiring a reduced bit rate of about 2 kpbs.

The data rates reported above refer to the transmission of color images and videos. However, some ROVs, such as the Ageotec models Pegaso and Perseo [15], can also transmit black and white video, which sometimes can provide better contrast than color streams. While it is true that black and white videos imply a lower data rate, we decided to design and evaluate the control system for the more demanding of the two cases, and therefore to consider the transmission of color videos in the computation of the minimum bit rate in each mode. Of course, this system would be able to support the transmission of black and white video streams as well.

Each of the modes above is supported by a different component of a multimodal communication system, which can autonomously choose the most suitable transmission technology depending on the channel conditions and the distance between the ROV and the controller. More specifically, Mode HD can be supported by an optical link which,

Table 1: System modes and modems employed

Mode	Manufacturer/model	Range	Bit rate [kbps] ^a
Mode 0	EvoLogics S2CR 18-34 [9]	3.5 km	13.9
Mode 1	EvoLogics S2CR 48-78 [9]	1 km	31.2 ^b
Mode 2	EvoLogics S2CM HS [9]	300 m	62.5 ^c
Mode 3	FAU Hermes modem [8]	120 m	87.7 ^d
Mode HD	Lumasys BlueComm [3]	20 m	5000 ^c

^a Bitrate and range as declared in the data sheets of the devices. They should be taken as an upper bound.

^b Worse results were achieved in Singapore’s warm shallow waters [21].

^c Recently released, no experimental results have been reported yet.

^d These values for the bitrate and range have been demonstrated in [8].

however, offers a limited coverage range of only a few meters. When the optical link cannot be used, the connection is enabled by one of the acoustic communication systems, thereby striking a trade-off between coverage range and bit rate. The FAU Hermes modem [8] achieves a bit rate of 87.7 kbps within a maximum communications range of 120 m, thereby supporting mode 3; the recently released EvoLogics [9] S2C M HS supports mode 2 via a bit rate of 62.5 kbps at a maximum distance of 300 m; Mode 1 is achieved through EvoLogics’ S2C R 48/78 modem, which supports communications at 31.2 kbps up to 1 km; finally, Mode 0 would be achieved by EvoLogics S2C R 18/34 modem. Table 1 provides a summary of the communications equipment employed in each mode and a few notes on the achieved performance. We stress that all the manufacturers declare to achieve the reported performance in shallow or very shallow water environments. In our scenario, the maximum distance that separates the controller and the ROV is about 180 m, therefore only Modes HD, 3 and 2 will be considered in this paper. In Section 3, we will detail how the communication stack implemented in the ROV and in the controller makes it possible to automatically switch among these modes. A different system setting, with different modems and ranges, is provided for the interested reader in [17], where we also argue that, given the current state of electro-magnetic and magneto-inductive communication equipment for underwater scenarios, the optical and acoustic technologies are the only feasible ones for our ROV control applications.

2.1 Early mode switching via signaling

Multimodal communication systems require a strategy to switch between different PHYs according to the channel conditions, e.g., to maximize the instantaneous throughput at any given time. For applications requiring a continuous flow of traffic through a point-to-point connection, a straightforward strategy is to quantize the use of any PHY down to a fixed amount of time, at the end of which the PHY choice is reevaluated. While a PHY is in use, the received power level over this PHY is continuously monitored: once a preset threshold is exceeded, the system switches to a different PHY at the beginning of the next PHY evaluation period. However, this system may not be sufficiently fast to react

at the speed at which the conditions of the communication vary [10]. Therefore, in this paper we also introduce an explicit PHY changing mechanism based on the transmission of specific control messages between the controller (or master) and the ROV (or slave). In particular, we prescribe that the master sends a packet in unicast to the slave in order to command an immediate PHY switch triggered by the received-power metric at the master node. At the price of a small overhead (which will be quantified in Section 4), the signaling mechanism relieves the slave from having to wait for the beginning of the next fixed transmission period before the PHY layer can be actually changed. This results in a much more agile behavior in the presence of optical communications, which offers very high throughput within a very limited coverage range, and must therefore be exploited as soon as it becomes available.

When the slave receives the signaling packet, it switches PHY according to the master’s indication. In addition, if the slave is also in signaling mode, it replies with another signaling packet, allowing the master to re-compute the power metric immediately after the switch. After the PHY switch command, the master expects to start receiving data over the new PHY. If this is not the case, after a Signaling Timeout (STO) interval of prescribed duration, the master signals the slave nodes, in broadcast, to switch to a more robust physical layer, in order to avoid losing an excessive number of transmissions and wasting the corresponding transmission energy. Both the STO and the slave signaling mode are useful for systems experiencing bursty traffic, where the collected time series of the received power do not provide sufficiently timely information about the channel conditions. A relevant example is when the slave is transmitting a burst of packets through the optical PHY, but a number of packets at the beginning of the burst are sent while the distance between the two nodes is too long in order to allow any packet reception, thus preventing the master from computing the power metric. Furthermore, without the STO, the system would lose all the subsequent incoming packets.

3. SIMULATION PARAMETERS AND SETTINGS

All simulation results have been obtained using a set of C/C++ libraries that simulate multimodal communications in underwater networks. They have been implemented as part of the DESERT Underwater v2 software [22] and released as open-source software [23]. The proposed scenario has two nodes: the ROV and its remote controller. The protocol stack implemented in each node is organized as follows:

- ROV CONTROL [17] application layer
- Either CSMA or TDMA MAC
- MULTI-STACK-CONTROLLER layer that coordinates multiple PHY, either with or without signaling
- ACOUSTIC PHY LAYER model that simulates the EvoLogics’ S2C M HS device [9]
- HERMES PHY LAYER [17] model that simulates the Hermes acoustic modem
- OPTICAL PHY LAYER [10] model that simulates optical communications.

The ROV CONTROL application layer has two primary operating modes: ROV and ROV-CONTROLLER. In the former, the module implements the ROV behavior, by receiving command packets, performing the request and sending monitoring packets to the controller. The ROV module is configured to continuously generate monitoring packets of length 1000 bytes at a fixed generation rate, preventing the node’s transmission queue from becoming empty. The ROV-CONTROLLER implements the ROV remote control behavior, by dispatching command packets to the ROV in order to control its position and to receive monitoring packets. The controller drives the ROV along the desired path by sending absolute movement commands in the form of a waypoint list. The path has been sampled in 101 way-points and the guard time between the transmission of subsequent waypoints has been set to $t_g = 2.5$ s. The command packets’ size is 125 bytes.

Given the presence of only two nodes, we employed the UDP transport layer, static routing and either the CSMA or the TDMA MAC protocol. The choice of two different MAC protocols will allow us to verify if the performance trends and conclusions stemming from the analysis of a single-PHY remote control system in [17] extend to the multimodal case. The mechanism used to switch among the different PHY layers conforms to the description given in Section 2.1. We set the STO to 3 s, as this value has resulted in the highest throughput in an extensive set of preliminary simulations.

In Section 4 we show the comparison of the system with and without signaling, in order to assess the benefits provided by this feature. A signaling packet has a size of 5 bytes. In our simulations, the OPTICAL PHY LAYER module [10] is configured as follows: transmission power equal to 100 W, 200 kHz of bandwidth,¹ 2-Mbps PHY bitrate, an SNR threshold to ensure correct reception equal to 20 dB, optical wavelength $\lambda = 532$ nm and a divergence angle $\theta = 0.5$ rad. In this configuration the optical transmission range is 14 m.

The HERMES PHY LAYER’s source level is 180.0 dB re μPa^2 at 1 m from the source. The transmission rate is 87768 bps, the carrier frequency is 375 kHz and the bandwidth is 76 kHz. The transmission range of the Hermes acoustic modem is 120 m.

Unfortunately no detailed information has been published on the performance of the new Evologics’ S2C M HS acoustic modem, therefore we employed the default DESERT ACOUSTIC PHY LAYER in order to simulate it. The modem’s source level is set to 177 dB re μPa^2 at 1 m from the source², whereas the carrier frequency and the bandwidth available for communications are 160 kHz and 80 kHz, respectively.

The threshold model employed in the master switching system is described in [10]. The switching thresholds are chosen so as to ensure the proper operation of each PHY technology while in use. For example, this means that the thresholds for switching from the Hermes modem to the optical modem and vice-versa depend on the conditions of the water in terms of turbidity and ambient light noise. Similar considerations apply to the acoustic PHYs. The power thresholds are reported in the following list:

- Evologics HS \rightarrow Hermes: 139.95 dB re μPa^2 at 1 m
- Hermes \rightarrow Evologics HS: 138.04 dB re μPa^2 at 1 m
- Hermes \rightarrow Optical Modem: 161.70 dB re μPa^2 at 1 m
- Optical Modem \rightarrow Hermes: $1.08 \cdot 10^{-8}$ W

In our simulations, the ROV moves at a speed of 1 m/s, at a depth of 40 m in a water column of 100 m, whereas the controller has fixed position and is deployed at a depth of 38.5 m. We implement the empirical underwater sound propagation and noise models in [24], with a spreading coefficient equal to 1.5 in the spreading loss component, no shipping activity and speed of wind of 1 m/s. The speed of sound under water is assumed to be constant and equal to 1500 m/s. The underwater speed of light is set to $2.25 \cdot 10^8$ m/s. For assessing the impact of the solar irradiance on the optical communications component of the multimodal control system, we assume environmental conditions that are typical of a coastal ocean scenario. In particular, the attenuation coefficient is set to $c = 0.4 \text{ m}^{-1}$, equally subdivided between the absorption coefficient a and the scattering coefficient b , where $c = a + b$. Furthermore, we assume the absence of clouds, and a solar zenith angle of 0 rad, which is obtained during solar noon at the equatorial line. In these conditions, the solar irradiance perceived by the controller is $1.9 \cdot 10^{-4} \text{ W/m}^2$.

4. RESULTS

In this section we analyze the system performance in order to assess which configuration is best for the remote control of an underwater vehicle over a wireless link in our scenario. In particular, we focus on the achievement of the minimum required bit rate for each mode (see Section 2), the speed of the switching between modes, the ROV’s deviation from the path commanded by the controller, and the signaling overhead, which is defined as the number of signaling bits sent divided by the total number of bits transmitted.

4.1 Results–CSMA MAC scheme

First we analyze the performance achieved by the control mechanism when using a CSMA MAC protocol without signaling for prompt switching. This configuration may be suboptimal, but entails a simplified system implementation, as there is no need to enable additional services such as localization and time synchronization between the controller and the ROV; moreover, no signaling overhead is required. However, the performance of the control system does not achieve the expected targets in terms of desired monitoring data throughput in each system mode defined in Section 2. The latter, in particular, can be observed from Fig. 1, which shows one realization of the instantaneous throughput achieved by the system as a function of the simulation time. The figure is focused on the part of the simulation where the ROV is closest to the controller (represented as a triangle centered at the bottom of the figure), which in turn triggers the shift from Mode 2 to 3 (around 275 s), then to Mode HD (at about 400 s), and back to 3 (about 430 s) and 2 (540 s). Three dashed lines mark the minimum throughput that should be achieved in Mode HD (red), Mode 3 (blue) and Mode 2 (green).

We observe that the throughput for the case of CSMA with no signaling, represented by a thin, dark-gray line, correctly remains around the prescribed level in Mode 2, but

¹These parameters correspond to our own understanding of the Lumasys BlueComm HAL optical transceiver, as its datasheet reports neither its transmission power nor its bandwidth.

²Value declared by the manufacturer.

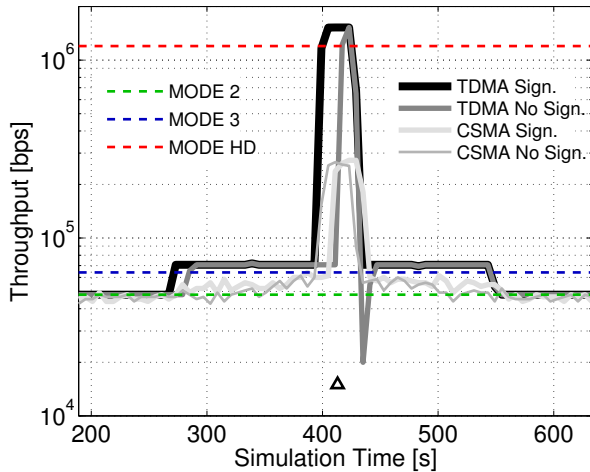


Figure 1: Throughput achieved by the four MAC and PHY switching configurations considered in this paper as a function of the simulation time.

fails to achieve the level prescribed by Mode 3, and cannot even exploit optical communications properly when it becomes available. The main reason for this is the lack of coordination between the transmissions of commands by the controller and the transmission of monitoring data by the ROV. There is a high chance that these transmissions take place while the other node is also transmitting, which results in significant packet losses. The resulting metrics are as follows: packet delivery ratio (PDR) of control packets: 84%; average path deviation: 2.0 m; path RMSE: 2.7 m; average throughput of 56.1 kbps; no signaling overhead.

We now turn to the case where the switching mechanism is employed to notify that the choice of the PHY should be changed. It turns out that this mechanism yields little if any significant improvement with respect to the case without signaling: in fact, the ROV deviation from the intended path gets smaller (on average, about 28% with respect to the case without signaling), but despite the faster PHY switch, the monitoring traffic requirement is not achieved, as can be seen from the light-gray line in Fig. 1. In particular, we note that the peak throughput during optical communications is negligibly higher than the maximum achieved in the no signaling case, and in any event it is one order of magnitude lower than the requirement of 1.4 Mbps. When TDMA is employed, the achieved throughput is generally much more stable and higher. Signaling helps TDMA improve the PHY switching efficiency as well. In particular, we note that the low value of the TDMA throughput around 440 m in the no signaling case (dark grey line) is due to a late switch, whereby the optical PHY technology is suboptimally employed beyond its coverage range. This causes the optical link to fade and the average throughput to decrease, before a link with the Hermes modem (the fastest of the two acoustic technologies considered here) is finally established at about 450 m. Such an event is prevented by the signaling mechanism (black line).

The behavior of the control system along the trajectory commanded by the controller is presented in Fig. 2 in terms of monitoring throughput versus ROV position, both in a

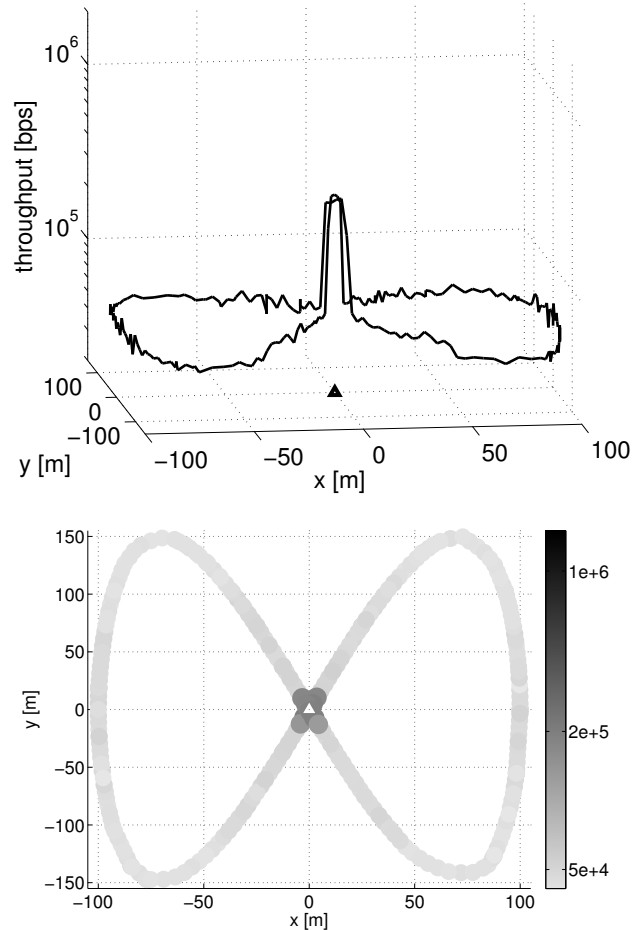


Figure 2: CSMA with signaling: 3D (top) and 2D projection (bottom) of the throughput against the position of the ROV along one lap.

3D plot (top pane) and in a 2D projection seen from above (bottom pane). In the latter, the performance metric is represented using gray-scale points, with a circle area and gray shade level proportional to the throughput values along that portion of the trajectory. The position of the remote controller is represented by a triangle. The PHY switch occurs correctly, however, the throughput of the monitoring traffic varies broadly in every mode and the optical throughput does not increase above 250 kbps. In the case of no signaling the system behavior is very similar, with the exception of a longer PHY switch time.

To summarize, the main reason for the monitoring performance degradation is the CSMA protocol configuration, in terms of listening and back-off timing which causes packet collision and deafness states. This setup can dramatically reduce the maximum throughput and the PDR of the control packets sent by the controller. The low control packet PDR is the main cause of ROV deviation from the desired path: the higher the PDR, the smaller the deviation. Due to this trade-off, the system cannot meet the monitoring traffic constraint. Other system performance figures are control packet PDR: 85%; average path deviation: 1.4 m; path RMSE:

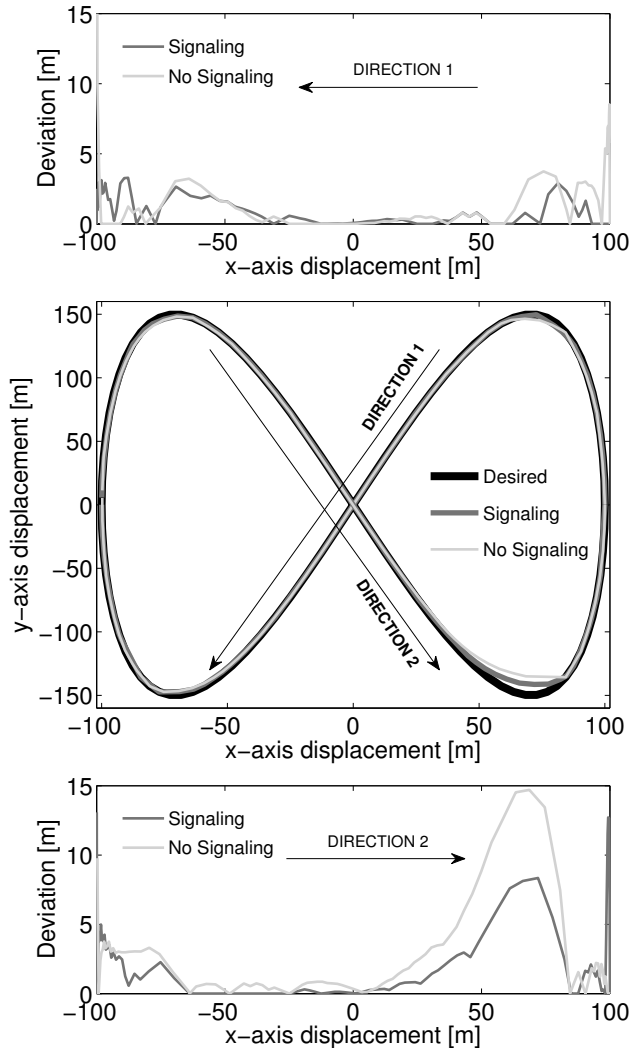


Figure 3: CSMA: route followed by the ROV and deviation from the desired route as a function of the position of the ROV along the x-axis.

2.1 m; average throughput: 57.9 kbps; signaling overhead: $3.3 \cdot 10^{-6}$.

A detailed analysis of the deviation of the ROV from the desired path is provided in Fig. 3 for the CSMA case. In particular, the middle pane shows a superimposition of the desired trajectory (black) to the actual ones followed by the ROV, both in the presence (dark gray) and in the absence (light gray) of signaling. The figure-of-eight trajectory has been split into two legs in order to make the analysis simpler. The first leg goes from point (100, 0) to point (-100, 0) following direction 1. The deviation of this part of the trajectory from the desired path is shown in the top pane. The second leg goes from (-100, 0) to (100, 0) following direction 2. The deviation of this trajectory from the wanted one is reported in the bottom pane.

We observe that the maximum path deviation is 15 m in the case of no signaling, and is suffered near point (70, -150), which corresponds to one of the farthest distances between the ROV and the controller. The maximum deviation de-

creases to about 12.5 m in the case of PHY switch with signaling, and is observed towards the end of the trajectory, when the ROV is almost back at its original position. Also in this case, a deviation peak (albeit slightly lower than in the no signaling case) is observed near the point (70, -150). The peaks are due to lack of reception of some waypoint, either due to errors over the signaling channel (in turn most likely due to untimely PHY switching) or due to deafness at the ROV induced by a ROV transmission. Either event makes the ROV lose some of the required waypoints along the route. When an ensuing waypoint is finally received, the ROV will then head towards the most recently received waypoint, and skip all lost ones. In the remaining portions of the path, the deviation is typically less than 5 m, and becomes larger when the distance between the ROV and the controller increases. The ROV, in both system configurations, follows the trajectory with very similar reliability. This confirms that the PHY signaling system does not provide significant advantages in terms of throughput or path deviation. We note that errors and deafness take place randomly in each realization of our simulation setup, and therefore the behavior of the ROV along a trajectory is not necessarily symmetric, nor identically equal to the realization shown in Fig. 3.

4.2 Results—TDMA MAC scheme

In this section, we discuss the performance of the multimodal ROV control system with a TDMA MAC layer. First of all, we note that our TDMA channel access mechanism subdivides time into frames, which in turn are divided into four time slots: a slot dedicated to the monitoring feedback from the ROV (of length t_{rov}), a guard time interval of length t_i , a slot dedicated to the control messages from the controller (of length t_{ctr}) and a second guard interval t_i . We stress that the slot durations and the guard interval are set so that both the ROV and the controller have sufficient time to send their monitoring and control packets, respectively. In particular, the ROV must send a large amount of data, and to do so it needs a time slot larger than the controller's. This has been achieved by setting $t_{rov} = 4.8$ s, $t_{ctr} = 0.8$ s and $t_i = 0.2$ s. We first consider the case where no signaling is employed by the PHY switching mechanism. The observed performance metrics are as follows; control packet PDR: 100%; average path deviation: 0.6 m; path RMSE: 1.50 m; average throughput: 83.4 kbps; signaling overhead = 0. The TDMA protocol provides two main advantages. First, no collisions and deafness occur, as the ROV correctly receives all the waypoints, thus following its path with a small deviation (the average path deviation is four times smaller than the CSMA case). Second, the system experiences a higher throughput, and consistently achieves the monitoring target in each control Mode, as seen from the bold gray line in Fig. 1. This configuration is not very reactive. Although the PHY switch occurs correctly, the observed delay causes a decrease of the measured throughput, as well as of the average throughput along the path. For instance, if the switch from the Hermes (acoustic) to the optical PHY occurs with a delay of 3 seconds, the system can transmit 3.3 Mb less than in the optimal case.

Employing the signaling mechanism to switch PHY solves this issue (black curve of Fig. 1). In this case, the performance of the control system improves even further as indicated by the following metrics; control PDR: 100%, av-

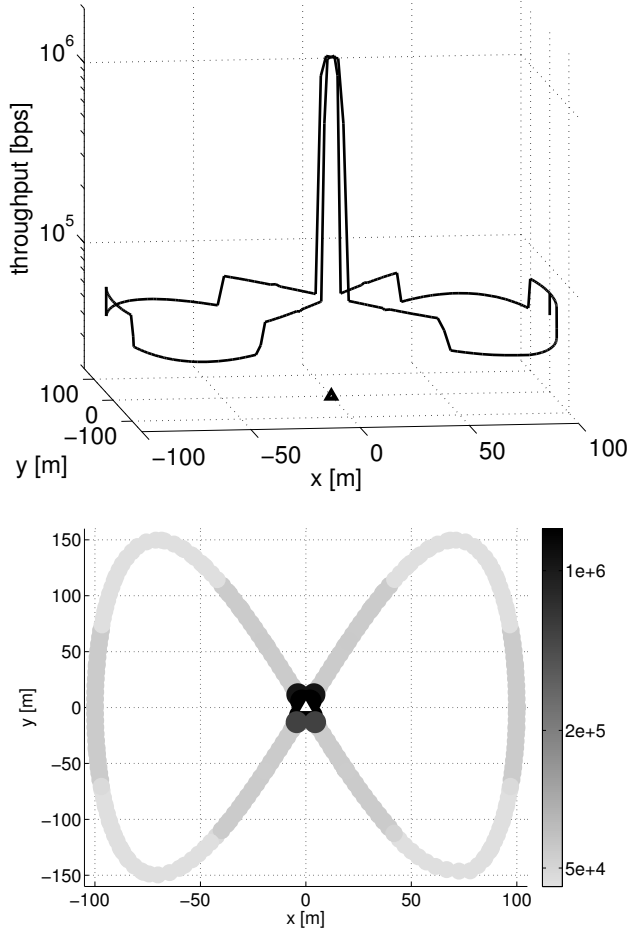


Figure 4: TDMA with signaling: 3D (top) and 2D projection (bottom) of the throughput against the position of the ROV along one lap.

erage path deviation: 0.2 m, path RMSE: 1.0 m, average throughput: 117.6 kbps, signaling overhead = $1.7 \cdot 10^{-6}$. For this case, we report the monitoring throughput versus the ROV position in Fig. 4, both in a 3D plot (top pane) and in a 2D projection (bottom). We observe that the switch occurs correctly, the monitoring traffic flows smoothly and constantly, and the bit rate targets in each mode are consistently achieved. In particular, the bottom pane shows that only the farthest portions of the trajectory have to fall back to Mode 2, whereas the sections immediately closer to the controller can already use Mode 3, and the points in its immediate proximity enjoy the high bit rate allowed by the optical connection. In the case of no PHY signaling the system behavior is very similar, but the switch among different PHYs is delayed, thus causing a performance loss.

The comparison of the ROV path deviation (top and bottom panes) against the commanded route (intermediate pane) is shown in Fig. 5. The maximum path deviation is 4 m in the case of no PHY signaling and 0.5 m in the case of PHY switch with signaling. The ROV, in both system configurations, follows the trajectory with significant reliability, and when the PHY signaling is active the deviation from the re-

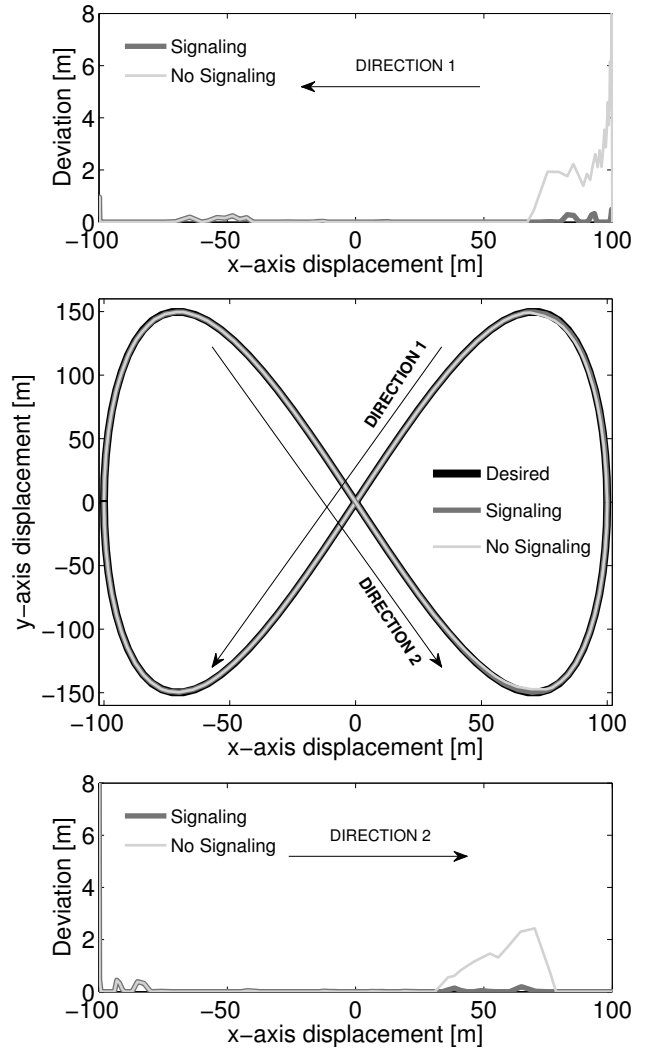


Figure 5: TDMA: route followed by the ROV and deviation from the desired route as a function of the position of the ROV along the x-axis.

quested path is almost zero. In this case, the PHY signaling technique provides a reduction of path deviation and a large improvement in terms of monitoring traffic, at the cost of a negligible signaling overhead.

5. CONCLUSIONS

In this paper, we demonstrated the effectiveness of a multimodal wireless remote control system for underwater mobile vehicles, by comparing the performance of different system configurations. The results show that the TDMA MAC layer is more robust than CSMA, in terms of both throughput and ROV deviation from the desired trajectory. This is due to the fact that coordinating the transmissions of the ROV and of the controller avoids the occurrence of deafness and collisions. This trend confirms the work presented in [17] and extends it to a multimodal case. In addition, we have shown the effectiveness of a PHY switching signaling mechanism, which makes moving from a PHY to another in the multimodal system faster and more reliable, at the

cost of a negligible overhead. Future work will expand the TDMA study to the case of multiple controlled entities and consider its implementation for a real-time case involving actual transceivers, in order to pave the way for the implementation in a real system. In addition, we plan to compare different system configurations, for instance by always sending command packets through the most robust PHY available, while the monitoring packets are sent through the one offering the best performance.

Acknowledgments

This work has been supported in part by the US Office of Naval Research under Grant no. N62909-14-1-N127, and by the European Commission through the 7th Framework Programme, AMAROUT II project, G.A. no. 291803.

6. REFERENCES

- [1] I. Vasilescu, K. Kotay, D. Rus, P. Corke, and M. Dunbabin, "Data collection, storage and retrieval with an underwater optical and acoustical sensor network," in *Proc. ACM Sensys*, San Diego, CA, Nov. 2005.
- [2] N. Farr, A. Bowen, J. Ware, C. Pontbriand, and M. Tivey, "An integrated, underwater optical/acoustic communications system," in *Proc. IEEE/OES OCEANS*, Sydney, Australia, May 2010.
- [3] "Lumasys, Inc.," Accessed: Sept. 2015. [Online]. Available: <http://www.lumasys.com/products.html>
- [4] "Ambalux high-bandwidth underwater transceiver," Accessed: Sept. 2015. [Online]. Available: <http://www.ambalux.com/underwater-transceivers.html>
- [5] "Wireless For Subsea Seatooth," accessed: Sept. 2015. [Online]. Available: <http://www.wfs-tech.com/index.php/products/seatooth/>
- [6] X. Che, I. Wells, G. Dickers, P. Kear, and X. Gong, "Re-evaluation of RF electromagnetic communication in underwater sensor networks," *IEEE Communications Magazine*, vol. 48, no. 12, pp. 143–151, December 2010.
- [7] B. Gulbahar and O. B. Akan, "A communication theoretical modeling and analysis of underwater magneto-inductive wireless channels," in *IEEE Trans. Wireless Commun.*, vol. 11, no. 9, Sep. 2012, pp. 3326–3334.
- [8] P.-P. Beaujean, J. Spruance, E. A. Carlson, and D. Kriel, "HERMES - A high-speed acoustic modem for real-time transmission of uncompressed image and status transmission in port environment and very shallow water," in *Proc. MTS/IEEE Oceans*, Québec City, Canada, Sep. 2008.
- [9] "Evologics underwater SC2R acoustic modem series," accessed: Sept. 2015. [Online]. Available: <http://www.evologics.de/en/products/acoustics/index.html>
- [10] F. Campagnaro, F. Favaro, F. Guerra, V. Sanjuan, P. Casari, and M. Zorzi, "Simulation of multimodal optical and acoustic communications in underwater networks," in *Proc. MTS/IEEE Oceans*, Genova, Italy, May 2015.
- [11] S. Basagni, L. Bölöni, P. Gjanci, C. Petrioli, C. A. Phillips, and D. Turgut, "Maximizing the value of sensed information in underwater wireless sensor networks via an autonomous underwater vehicle," in *Proc. IEEE INFOCOM*, Toronto, Canada, Apr. 2014.
- [12] C. Moriconi, S. Betti, M. Tabacchiera, and G. Cupertino, "Hybrid, short range, underwater data channel," in *Proc. MTS/IEEE Oceans*, Genova, Italy, May 2015.
- [13] FMC Technologies, "ROV Systems Comparison," Accessed: September, 2014. [Online]. Available: <http://www.fmctechnologies.com/en/SchillingRobotics/Solutions/Schilling-ROV-Systems.aspx>
- [14] Submarine Manufacturing and Products, "Product Datasheet, ROV-1000-Model," Accessed: October, 2014. [Online]. Available: <http://www.smp-ltd.co.uk/tcpdf/datasheets/ROV-1000-Model.pdf>
- [15] Ageotec, "ROV & UNDERWATER TECHNOLOGIES," Accessed: Sept., 2015. [Online]. Available: <http://www.ageotec.com/products/rov-underwater-technologies/>
- [16] Woods Hole Oceanographic Institution, "Autonomous Underwater Vehicles," Accessed: Sept., 2015. [Online]. Available: <http://www.whoi.edu/main/auvs>
- [17] F. Campagnaro, F. Favaro, P. Casari, and M. Zorzi, "On the feasibility of fully wireless remote control for underwater vehicles," in *Proc. Asilomar Conf. SS&C*, Pacific Grove, CA, Nov. 2014.
- [18] F. M. Raimondi, M. Trapanese, V. Franzitta, A. Viola, and A. Colucci, "A innovative semi-immergible USV (SI-USV) drone for marine and lakes operations with instrumental telemetry and acoustic data acquisition capability," in *Proc. MTS/IEEE Oceans*, Genova, Italy, May 2015.
- [19] N. A. Cruz, B. M. Ferreira, O. Kebkal, A. C. Matos, C. Petrioli, R. Petroccia, and D. Spaccini, "Investigation of underwater acoustic networking enabling the cooperative operation of multiple heterogeneous vehicles," *Marine Technology Society Journal*, vol. 47, no. 2, pp. 43–58, 2013.
- [20] F. Campagnaro, "Design of a wireless remote control for underwater equipment," Master's thesis, University of Padova, Italy, 2014. [Online]. Available: <http://tesi.cab.unipd.it/46709/1/MasterThesis.pdf>
- [21] E. Haggmann, J. Maye, and A. Breitenmoser, "Underwater acoustic communications in warm shallow water channels," 2006, accessed: Sept. 2015. [Online]. Available: <http://scholarbank.nus.edu.sg/handle/10635/27859>
- [22] P. Casari *et al.*, "Open-source suites for the underwater networking community: WOSS and DESERT Underwater," *IEEE Network, special issue on "Open Source for Networking: Development and Experimentation"*, vol. 28, no. 5, pp. 38–46, Sep. 2014.
- [23] "DESERT Underwater github repository.," accessed: Sept. 2015. [Online]. Available: https://github.com/uwsignet/DESERT_Underwater
- [24] M. Stojanovic, "On the relationship between capacity and distance in an underwater acoustic communication channel," *ACM Mobile Comput. and Commun. Review*, vol. 11, no. 4, pp. 34–43, Oct. 2007.